

## **Supplementary information**

### **Mapping the structure of amyloid nucleation precursors by protein engineering kinetic analysis**

David Ruzafa<sup>1</sup>, Lorena Varela<sup>1,‡</sup>, Ana I. Azuaga, Francisco Conejero-Lara<sup>\*</sup>, Bertrand Morel<sup>\*</sup>

Departamento de Química Física e Instituto de Biotecnología, Facultad de Ciencias, Universidad de Granada, 18071 Granada, Spain

<sup>‡</sup>Present address: Department of Biochemistry, University of Oxford, South Parks Road, Oxford, OX1 3QU, United Kingdom

<sup>1</sup>These authors contributed equally to this work.

\*Correspondence should be addressed to F.C.-L. or B.M.; e-mail addresses: conejero@ugr.es, bmorel@ugr.es; tel.: +34 958 242371; fax: +34 958 272879.

## Text S1:

### Determination of initial rates of growth

In this study, initial rates of growth of amyloid structure were calculated by fitting the initial region of the ThT kinetics curves using a double exponential function:

$$y = y_0 + A_1 \cdot e^{-k_1 t} + A_2 \cdot e^{-k_2 t} \quad (1)$$

The initial slope of the ThT curves was then accurately calculated from the resulting fitting parameters as:

$$r_0 = \left( \frac{dy}{dt} \right)_{t \rightarrow 0} = A_1 \cdot k_1 + A_2 \cdot k_2 \quad (2)$$

The fit of the initial ThT curve (Figure S1) is only used for extrapolation purposes and only the initial slope (extrapolated to time zero) is considered. This operational extrapolation procedure allowed us an accurate determination of the initial slopes of the ThT curves and avoided the assumption of any time interval in the kinetics to define an initial aggregation rate.

Another alternative method of the initial slope was also tested by calculating the first derivative of the kinetic trace and extrapolated it to time zero. As shown in Table S1, the results obtained by the two procedures are identical.

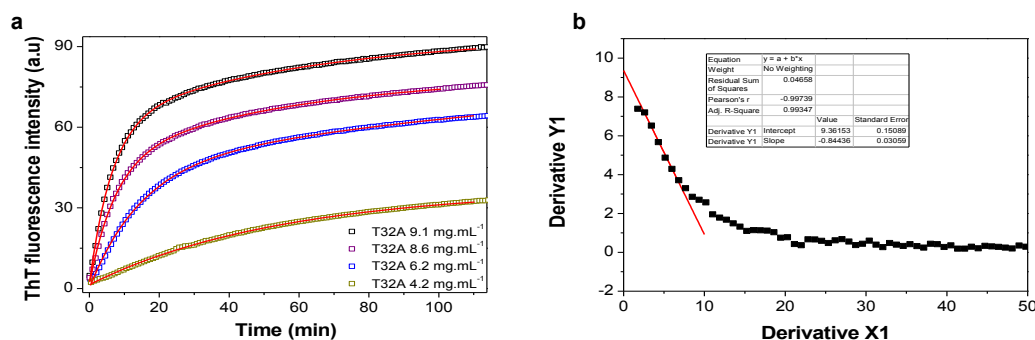


Figure S1: (a) Aggregation kinetics curves of T32A-N47A obtained from ThT fluorescence experiments. Symbols represent the experimental data and the continuous lines correspond to the best fit to equation 1. (b) First derivative of the ThT kinetics curve obtained for T32A-N47A (9.1 mg.mL<sup>-1</sup>) is represented in black squares. The tangent of the maximum decay is shown as the red line.

Concentration (mg.mL <sup>-1</sup> )	Equation 2	First derivative
9.1	9.80	9.36
8.6	6.70	6.82
6.2	3.28	3.25
4.2	0.65	0.66

Table S1: Initial rates obtained from ThT aggregation kinetics performed at different protein concentrations using the two methods described.

**Table S2.** Thermodynamic parameters of the equilibrium thermal unfolding of N47A Spc-SH3 and the double mutants measured by DSC in 0.1 M Glycine, 0.1 M NaCl pH 3.2.

Mutant	$T_m$ (°C)	$\Delta H_m$ (kJ.mol <sup>-1</sup> )
N47A <sup>a</sup>	51.2 ± 0.1	152.1 ± 0.4
N47A-L10A	30.3 ± 0.1	77.0 ± 0.5
N47A-R21D	53.5 ± 0.1	155.4 ± 0.3
N47A-K27A	46.7 ± 0.1	129.5 ± 0.6
N47A-T32A	41.6 ± 0.1	108.8 ± 0.2
N47A-N38A	38.6 ± 0.1	101.3 ± 0.3
N47A-K43A	43.9 ± 1.0	60.9 ± 4.2
N47A-V46A	42.3 ± 0.1	113.7 ± 0.4
N47A-D48G	55.7 ± 0.1	164.1 ± 0.4
N47A-V53A	54.5 ± 3.1	61.1 ± 6.7
N47A-A56G	46.1 ± 0.1	145.5 ± 0.4
N47A-V58A	56.1 ± 2.8	54.3 ± 4.8

Values of the unfolding temperature ( $T_m$ ) and enthalpy change ( $\Delta H_m$ ) have been obtained by two-state analysis of the DSC unfolding transitions. The errors have been estimated from the fittings as 95% confidence intervals for each parameter.

<sup>a</sup>: Data taken from Morel *et al.*,<sup>1</sup>.

**Figure S2. DSC experiments of N47A and the double mutants of Spc-SH3 domain.**

Experiments were carried out at low protein concentration in 0.1 M Gly, 0.1 M NaCl pH 3.2. Symbols represent the experimental data and the lines correspond to the best fit using the two-state unfolding model. For sake of clarity, experimental data of N47A mutant is shown in open squares and the best fit using the two-state unfolding model in dashed lines.

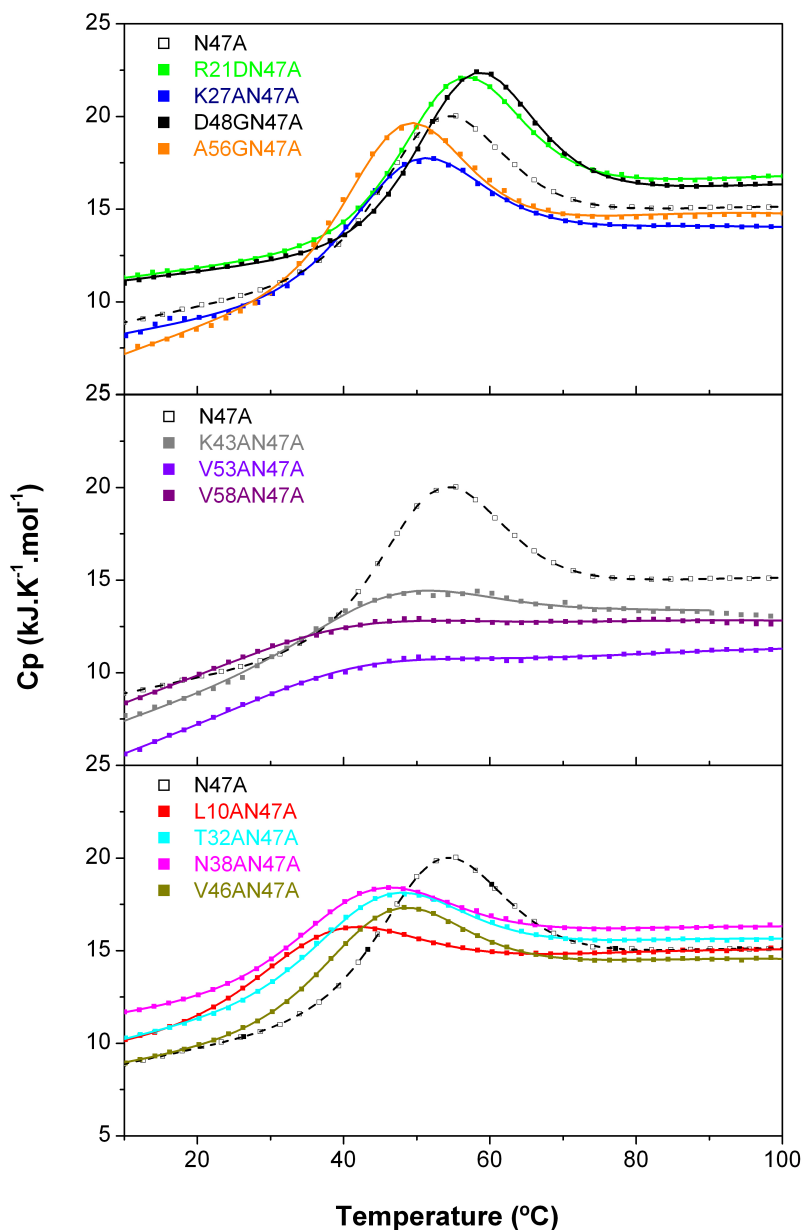


**Figure S3.** Aggregation kinetics at 37 °C of the double mutants and the N47A mutant followed by scattering intensity.

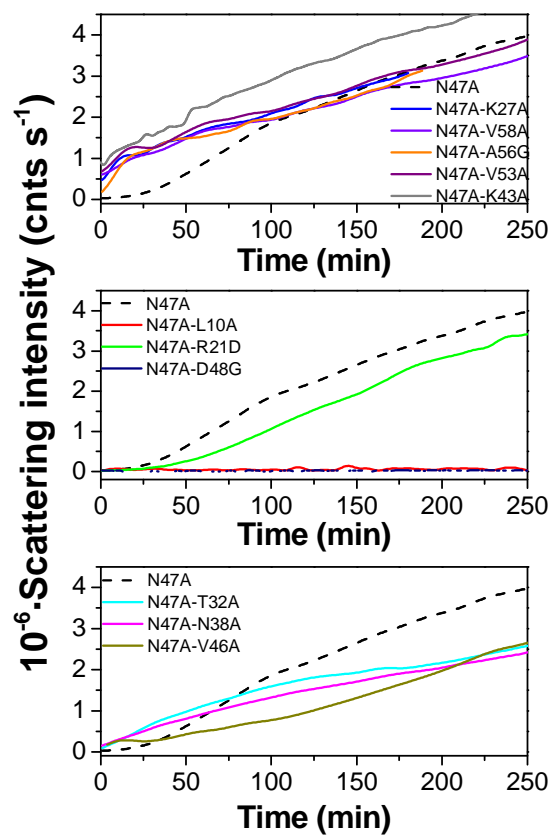


**Figure S4.** Time evolution of the apparent hydrodynamic radii ( $R_h$ ) for the two smallest peaks in the particle size distributions measured by DLS during the course of fibrillation of the N47A and the double mutants of Spc-SH3 domain. The continuous lines represent the best fit of the time dependence of the apparent  $R_h$  using a logistic sigmoidal function.

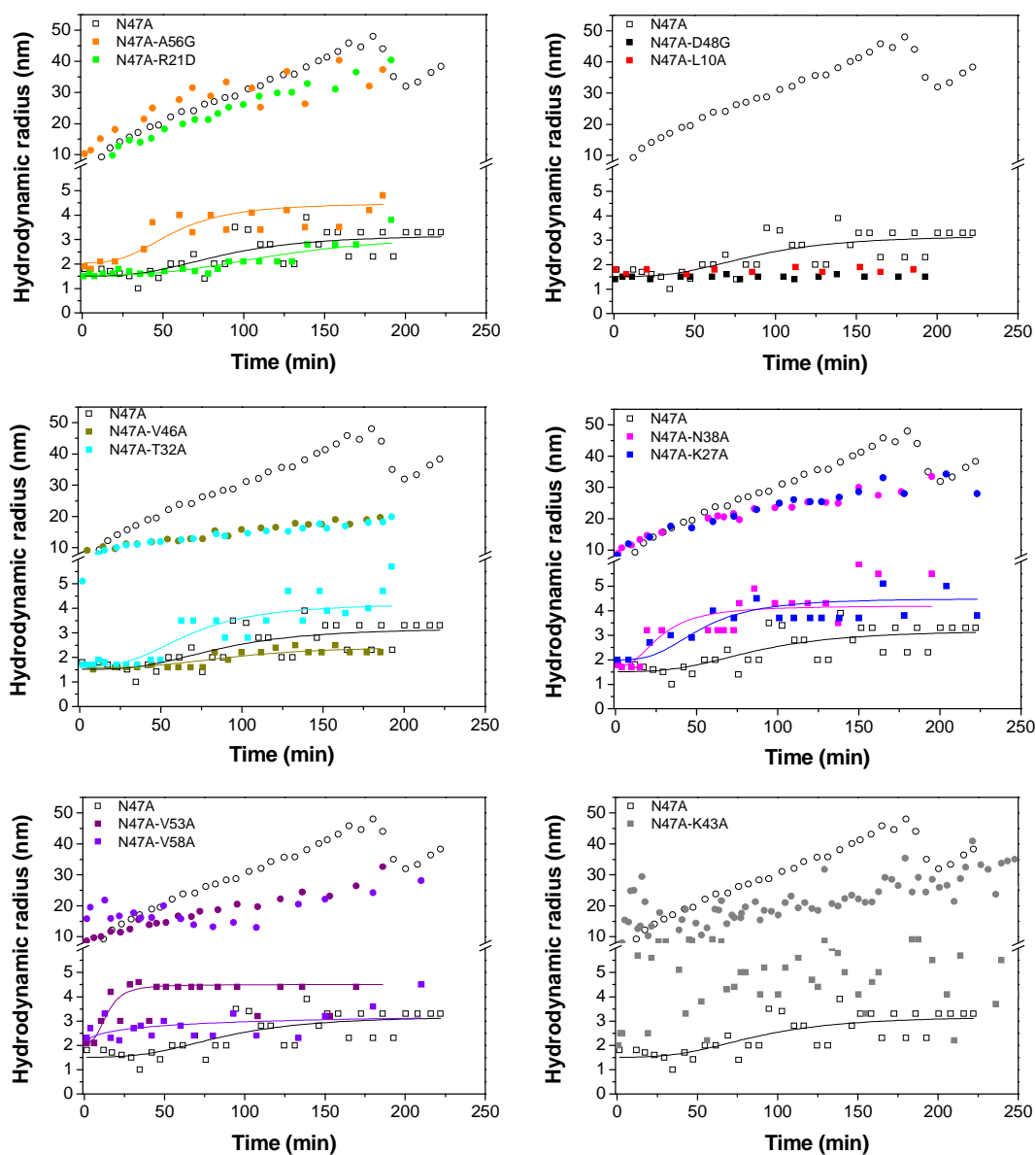


**Figure S5.** The energy changes produced by the different mutations in the native-state stability do not correlate with the changes in the rates of nucleation. Plot of  $\Delta G_I$  versus  $\Delta G_{N-U}$ .<sup>a</sup> Determined from aggregation kinetics studied in the presence of 0.2 M NaCl.

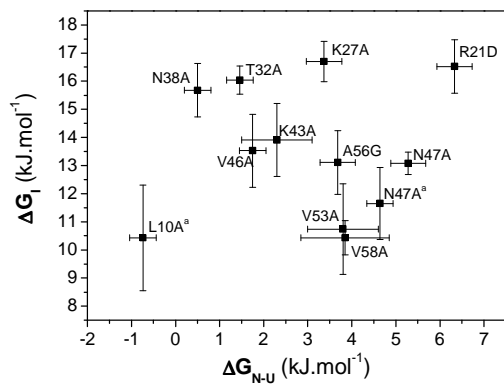
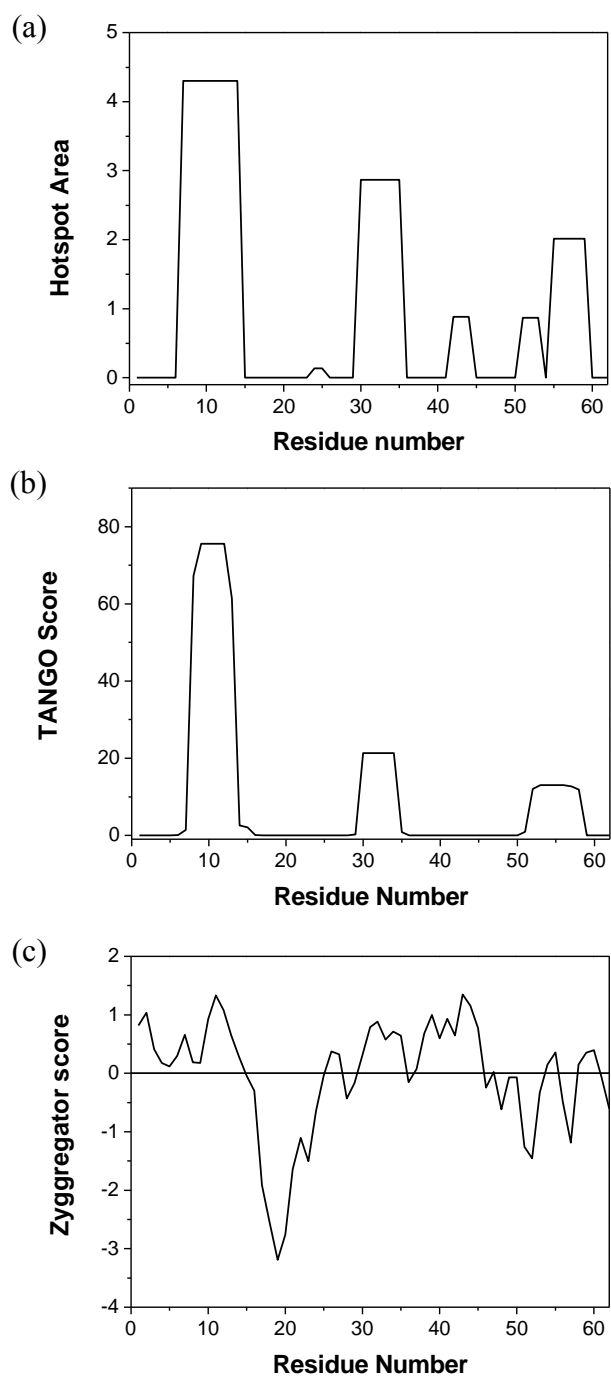


**Figure S6.** The aggregation propensity of the primary sequence of N47A Spc-SH3 domain predicted by the algorithms (a) Aggrescan <sup>2</sup> (b) TANGO <sup>3</sup> and (c) Zyggregator

4





## References

1. Morel, B., Varela, L., Azuaga, A.I. & Conejero-Lara, F. Environmental Conditions Affect the Kinetics of Nucleation of Amyloid Fibrils and Determine Their Morphology. *Biophys. J.* **99**, 3801-3810 (2010).
2. Conchillo-Sole, O. et al. AGGRESCAN: a server for the prediction and evaluation of "hot spots" of aggregation in polypeptides. *BMC Bioinformatics* **8**, 65 (2007).
3. Fernandez-Escamilla, A.M., Rousseau, F., Schymkowitz, J. & Serrano, L. Prediction of sequence-dependent and mutational effects on the aggregation of peptides and proteins. *Nat. Biotechnol.* **22**, 1302-1306 (2004).
4. Tartaglia, G.G. & Vendruscolo, M. The Zygggregator method for predicting protein aggregation propensities. *Chem. Soc. Rev.* **37**, 1395-1401 (2008).